Andrographis paniculata ameliorates estrogen deficiency-related osteoporosis by directing bone marrow mesenchymal stem cell fate

Qian Song[1#], Dongming Zhou[2#], Jianyang Du[3#], Tao Li[4], Xueyu He[5], Jianxiong Wang[6], Aijun Chao[1], Bingbing Yu[7,8], Chunyan Shan[9]

[1]Department of Osteo-internal Medicine, Tianjin Hospital, Tianjin, China; [2]Department of Traumatic Orthopedics, The First Affiliated Hospital of Baotou Medical College, Inner Mongolia University of Science and Technology, Baotou, Inner Mongolia Autonomous Region, China; [3]Department of Neurosurgery, Shandong Provincial Hospital Affiliated to Shandong First Medical University, Jinan, China; [4]Department of Orthopedics, Sun Yat-sen Memorial Hospital, Sun Yat-sen University, Shenshan Central Hospital, Shanwei, China; [5]Department of Pediatrics, Sun Yat-sen Memorial Hospital, Sun Yat-sen University, Shenshan Central Hospital, Shanwei, China; [6]Department of Endocrinology, Tianjin Hospital, Tianjin, China; [7]Department of Orthopedics, The Fifth Affiliated Hospital of Guangzhou Medical University, Guangzhou, China; [8]Key Laboratory of Biological Targeting Diagnosis, Therapy and Rehabilitation of Guangdong Higher Education Institutes, The Fifth Affiliated Hospital of Guangzhou Medical University, Guangzhou, China; [9]Department of Nephrology, Tianjin Medical University, Chu Hsien-I Memorial Hospital & Tianjin Institute of Endocrinology, NHC Key Laboratory of Hormones and Development, Tianjin Key Laboratory of Metabolic Diseases, Tianjin, China

Contributions: (I) Conception and design: Q Song, C Shan, B Yu; (II) Administrative support: Q Song; (III) Provision of study materials: T Li, D Zhou; (IV) Collection and assembly of data: X He; (V) Data analysis and interpretation: J Wang, A Chao; (VI) Manuscript writing: All authors; (VII) Final approval of manuscript: All authors.

[#]These authors contributed equally to this work.

Correspondence to: Qian Song. Department of Osteo-internal Medicine, Tianjin Hospital, Tianjin 300200, China. Email: songqian66882020@163.com; Bingbing Yu. Department of Orthopedics, The Fifth Affiliated Hospital of Guangzhou Medical University, Guangzhou, China. Email: gywyjzwkybb@163.com; Chunyan Shan. Department of Nephrology, Tianjin Medical University, Chu Hsien-I Memorial Hospital & Tianjin Institute of Endocrinology, NHC Key Laboratory of Hormones and Development, Tianjin Key Laboratory of Metabolic Diseases, Tianjin, China. Email: chunyanshan@hotmail.com.

Background: Although *Andrographis paniculata* (AP) exhibits various biological functions such as anticancer, anti-inflammatory, antimalarial, antimicrobial, antioxidant, cardioprotective and immunomodulatory, its role in estrogen deficiency-related osteoporosis remains unclear.

Methods: Ovariectomy (OVX)-induced estrogen deficiency-related osteoporotic mouse models and sham mouse models were established using 8-week-old female C57BL/6J mice. Micro-computed tomography (µCT) scanning was performed to assess the skeletal phenotype. The differentiation potential of bone marrow mesenchymal stem cells (BMSCs) from the OVX and sham groups was assessed by osteogenic or adipogenic induction medium *in vitro*. To verify the effects of AP, alizarin red S (ARS) staining, alkaline phosphatase (ALP) staining and oil red O (ORO) staining, reverse transcription assay and quantitative real-time polymerase chain reaction were applied to detect the lineage differentiation ability of BMSCs.

Results: µCT scanning showed that AP treatment attenuated the osteoporotic phenotype in OVX-induced estrogen deficiency-related osteoporotic mice. The results of ARS staining, ALP staining, ORO staining and quantitative real-time polymerase chain reaction indicated that BMSCs from OVX-induced osteoporotic mice displayed a significant reduction in osteogenic differentiation and an increase in adipogenic differentiation, which could be reversed by AP treatment.

Conclusions: Our findings suggested that AP regulated the differentiation potential of BMSCs and ameliorated the development of estrogen deficiency-related osteoporosis, which might be an effective therapeutic method for estrogen deficiency-related osteoporosis.

Keywords: *Andrographis paniculata* (AP); bone loss; bone marrow mesenchymal stem cells (BMSCs); osteoporosis

Introduction

Bone marrow mesenchymal stem cells (BMSCs) are non-hematopoietic stem cells and progenitor cells that have the potential to differentiate into various cell types, including osteoblasts, adipocytes, and chondrocytes (1,2). BMSCs are characterized by their abundance, high capacity for self-renewal, pluripotency, weak immunogenicity, and ease of transfection (3), which makes them as an ideal source of stem cells for transplantation and they are broadly used for the treatment of bone-related diseases (4). There are multiple factors that regulate the osteogenic and adipogenic differentiation of bone marrow mesenchymal stem cells, including ageing, epigenetic modifications, source, autophagy, inflammatory environment and intracellular signals (5-10). The balance between osteogenesis and adipogenesis of BMSCs plays a vital role in maintaining bone homeostasis and is a determinant in the development of osteoporosis (11). For example, with aging, BMSCs exhibit a reduction in the ability to differentiate into osteoblasts rather than adipocytes, resulting in obvious bone loss and marked fat accumulation in the bone marrow (12,13). As well, estrogen deficiency-related osteoporosis, coupled with increased bone marrow fat, is caused by the imbalance between osteoblast and adipocyte differentiation of BMSCs.

Therefore, novel therapeutic methods that decide the fate of BMSCs need to be further investigated.

Highlight box

Key findings
- AP exerted the anti-osteoporotic functions by regulating the osteogenesis and adipogenesis of BMSCs.

What is known and what is new?
- AP treatment prevented both the bone loss and impaired osteogenesis of BMSCs in estrogen deficiency-related osteoporotic mice.
- AP also reversed the increased adipogenesis of BMSCs from osteoporotic mice.

What is the implication, and what should change now?
- The study strongly suggested that AP might prevent the development of osteoporosis by regulating the osteogenesis and adipogenesis of BMSCs and might be an effective therapeutic method for estrogen deficiency-related osteoporosis.

Andrographis paniculata (AP) is a prioritized medicinal plant that belongs to the family Acanthaceae and is widely distributed in southern Asia (14). It has a very bitter taste and is known as the "King of bitters". The leaves and roots are usually applied for "cold property" to remove body heat and dispel toxins from the body. AP is often used in Indonesia for treating diabetes (15). Research has shown that AP exhibits biological activities, such as antidiabetic, anti-angiogenetic, antibacterial, anticancer, anti-inflammatory, antimalarial, antioxidant, and hepatoprotective activities (16). Its biological functions are related to bioactive compounds, including andrographolide, dehydroandrographolide, neoandrographolide, and deoxyandrographolide. AP is broadly used for the treatment of liver diseases, fever, common cold, acute diarrhea, hypertension, chicken pox, leprosy, hepatitis and malaria (17). Research has investigated whether AP could be used to prevent neutrophil accumulation and infiltration (18), and it has been demonstrated to enhance osteogenesis and chondrogenesis of mesenchymal stem cells from human suprapatellar fat pad tissues (19). However, the role of AP in the differentiation of BMSCs and the development of osteoporosis, especially estrogen deficiency-related osteoporosis, remains unclear.

In our study, we investigated the functions of AP in the osteogenesis and adipogenesis of BMSCs and the development of estrogen deficiency-related osteoporosis. We present the following article in accordance with the ARRIVE reporting checklist (available at https://atm.amegroups.com/article/view/10.21037/atm-22-1121/rc).

Methods

Isolation, culture and drug treatment

Following the isolation of murine BMSCs, the cells were cultured to the third passage as previously described (20). BMSCs were cultured in the medium containing α-MEM medium (Gibco, USA), 20% fetal bovine serum (FBS; ThermoFisher, USA), 2 mM L-glutamine (Invitrogen, USA), 100 U/mL penicillin and 100 U/mL streptomycin (Invitrogen, USA). The cells were maintained in an atmosphere of 5% CO_2 at 37 ℃. BMSCs at the third passage were used for further analysis. AP reagent was

Table 1 Primers used for qRT-PCR amplification

Gene	Primer sequence (5' to 3')
Runx2 (mouse)	F: ACTTCCTGTGCTCCGTGCTG
	R: TCGTTGAACCTGGCTACTTGG
Osterix (mouse)	F: ACCAGGTCCAGGCAACAC
	R: GCAAAGTCAGATGGGTAAGTAG
ALP (mouse)	F: CGTCTCCATGGTGGATTATGC
	R: TGGCAAAGACCGCCACAT
Pparg (mouse)	F: GACCACTCGCATTCCTTT
	R: CCACAGACTCGGCACTCA
Fabp4 (mouse)	F: AAATCACCGCAGACGACA
	R: CACATTCCACCACCAGCT
LPL (mouse)	F: GGGAGTTTGGCTCCAGAGTTT
	R: TGTGTCTTCAGGGGTCCTTAG
β-actin (mouse)	F: CTGTCCCTGTATGCCTCTG
	R: TGATGTCACGCACGATTT

qRT-PCR, quantitative real-time polymerase chain reaction; *Runx2*, runt-related transcription factor 2; *ALP*, alkaline phosphatase; *Pparg*, peroxisome proliferator activated receptor-g; *Fabp4*, fatty acid binding protein 4; *LPL*, lipoprotein lipase.

purchased from Sigma Aldrich, USA. The cells were treated with AP at 5, 10 and 20 µM, respectively.

Osteogenic differentiation assay

To induce osteogenic differentiation, the BMSCs were maintained in osteogenic induction medium (α-MEM supplemented with 10% FBS, 100 IU/mL penicillin and 100 µg/mL streptomycin, 10^{-8} M dexamethasone, 10^{-2} M β-glycerophosphate and 50 µg/mL L-ascorbic acid) for 14 days. The medium was replaced every 3 days.

Adipogenic differentiation assay

To induce adipogenesis, the BMSCs were maintained in adipogenic induction medium (α-MEM supplemented with 10% FBS, 100 IU/mL penicillin and 100 µg/mL streptomycin, 10^{-8} M dexamethasone and 6 ng/mL insulin) for 16 days. The medium was replaced every 3 days.

Alizarin Red S (ARS) staining

ARS staining was applied to assess mineralization after 14 days of osteogenic differentiation. BMSCs were washed three times with phosphate-buffered saline (PBS) to remove medium and fixed with 4% paraformaldehyde (PFA) for 20 min at room temperature. The cells were then stained with 1% ARS (Sigma, USA) for 20 min. Quantitative parameters of the mineralized areas were analyzed as previously reported (21). Finally, the stained cells were examined using an inverted microscope (Nikon, Japan).

Alkaline phosphatase (ALP) staining

ALP staining was applied to assess the osteogenic differentiation of BMSCs. BMSCs were washed twice with PBS, and ALP staining was performed according to the protocol previously reported (21). Finally, the stained cells were examined using an inverted microscope (Nikon, Japan).

Oil Red O (ORO) staining

ORO staining was conducted to detect the lipid droplet formation of BMSCs. ORO staining solution was prepared using 0.5 g ORO powder (Sigma, USA) and 100 mL of isopropanol. The solution was diluted with distilled water at the ratio of 3:2 and regarded as the working solution. The cells were washed three times with PBS to remove medium, and fixed with 4% PFA for 20 min at room temperature. The cells were stained with the ORO working solution for 15 min. The positive area was observed and analyzed.

RNA isolation and quantitative real-time polymerase chain reaction (qRT-PCR) assay

The TRIzol reagent (Life Technologies, USA) was added to the samples and total RNA was prepared according to the manufacturer's instructions (22). Then, reverse transcription assay and qRT-PCR assay were applied using Reverse Transcriptase (ABI, USA) and SYBRGreen qPCR Master Mix (Roche, Switzerland). The mRNA expression levels of genes were analyzed by the comparative cycle threshold method using *GAPDH* as control. The primers used for qRT-PCR amplification are listed in *Table 1*.

Animals and establishment of estrogen deficiency-induced osteoporotic model

All animals were purchased from the Qinhuangdao Lvjia Agricultural Science and Technology Development Co., Ltd., China. All animals were housed under specific

pathogen-free conditions (22 ℃, 50–55% humidity, and 12 h light/dark cycles) with food and water easily accessible. The 80 8-week-old female C57/BL6 mice were randomly divided into four groups (20 per group): sham group, ovariectomy (OVX) group, OVX + 50 mg/kg AP group and OVX + 100 mg/kg AP group. The OVX-induced estrogen deficiency-related osteoporotic mouse model was established by bilateral OVX. AP was administered via oral gavage. After 8 weeks, the mice were humanely killed and their femurs were obtained for micro-computed tomography (μCT) scanning. Animal experiments were performed under a project license (No. 2021121) granted by the Ethics Committee of Tianjin Hospital, in compliance with institutional guidelines for the care and use of animals.

Micro-computed tomography analysis

Trabecular bone tissues obtained from the femurs of mice and were scanned by μCT (SCANCO Medical, Switzerland) using 10.5-μm voxel resolution. Three-dimensional morphological parameters, including bone volume/tissue volume (BV/TV), trabecular number (Tb.N), trabecular thickness (Tb.Th) and trabecular separation (Tb.Sp) were obtained and analyzed.

Statistical analysis

Data were analyzed using Graphpad and the results shown as mean ± SD. Student's *t*-test was used to compare differences between groups. Comparisons of multiple groups were made using one-way ANOVA. All experiments were repeated at least three times, and representative experiments are shown. Data were considered significant at $P<0.05$.

Results

Effect of AP on accelerated bone loss in estrogen deficiency-related osteoporotic mice

We used OVX-induced estrogen deficiency-related osteoporotic mice to investigate whether AP can ameliorate osteoporosis. After 8 weeks, the trabecular bone tissues were obtained from the femurs of mice in the OVX, OVX + 50 mg/kg AP and OVX + 100 mg/kg AP groups and scanned by μCT, which showed that compared with the sham group, the BV/TV and Tb.N were much lower in the OVX group, and had been reversed after 50 mg/kg AP and 100 mg/kg AP treatment (*Figure 1A,1B*). The results also

showed that Tb.Th and trabecular separation Tb.Sp in the OVX group were much higher than in sham group, and had been reduced in the OVX + 50 mg/kg AP group and OVX + 100 mg/kg AP group (*Figure 1C,1D*). These results verified the characteristics of accelerated bone loss in OVX-induced estrogen deficiency-related osteoporotic mice and showed that it could be counteracted by AP treatment.

### Isolation and characterization of BMSCs

To assess the identities of the isolated BMSCs, they were characterized by phenotype analysis. The BMSCs were morphologically defined by a fibroblast-like appearance (*Figure 2A*). ARS, ALP and ORO staining confirmed that BMSCs could be induced into osteoblasts and adipocytes after osteogenic and adipogenic differentiation induction (*Figure 2B-2D*).

Effect of AP on decreased mineralization capability of BMSCs from osteoporotic mice

BMSCs play key roles in bone homeostasis and regeneration, and reduced osteogenic ability of BMSCs is critical for osteoporosis (23-25). To directly assess the role of AP in the osteogenic potential of BMSCs, those from the OVX mice were isolated and treated with AP at different concentrations, and then cultured in osteogenic-inducing medium for 14 days. As exhibited by ARS staining and ALP staining, BMSCs from the sham group demonstrated reduced osteogenic differentiation, with weaker mineralization capability and reduced areas of mineralized nodules (*Figure 3A-3D*). Importantly, compared with the sham group, the BMSCs from the OVX group were dramatically defective in their mineralization capability, as quantified by ALP activity and quantitative parameters of ARS staining (*Figure 3A-3D*). Notably, the results of ARS and ALP staining showed that the mineralization ability of BMSCs from osteoporotic mice was increased by AP administered at 5, 10 and 20 μM, which suggested that AP treatment substantially rescued the osteogenic decline of BMSCs from OVX mice (*Figure 3A-3D*). The results proved that AP reversed the decreased mineralization capability of BMSCs from osteoporotic mice.

Effect of AP on the expression of osteogenic marker genes of BMSCs from osteoporotic mice

During the osteogenic induction process, several genes
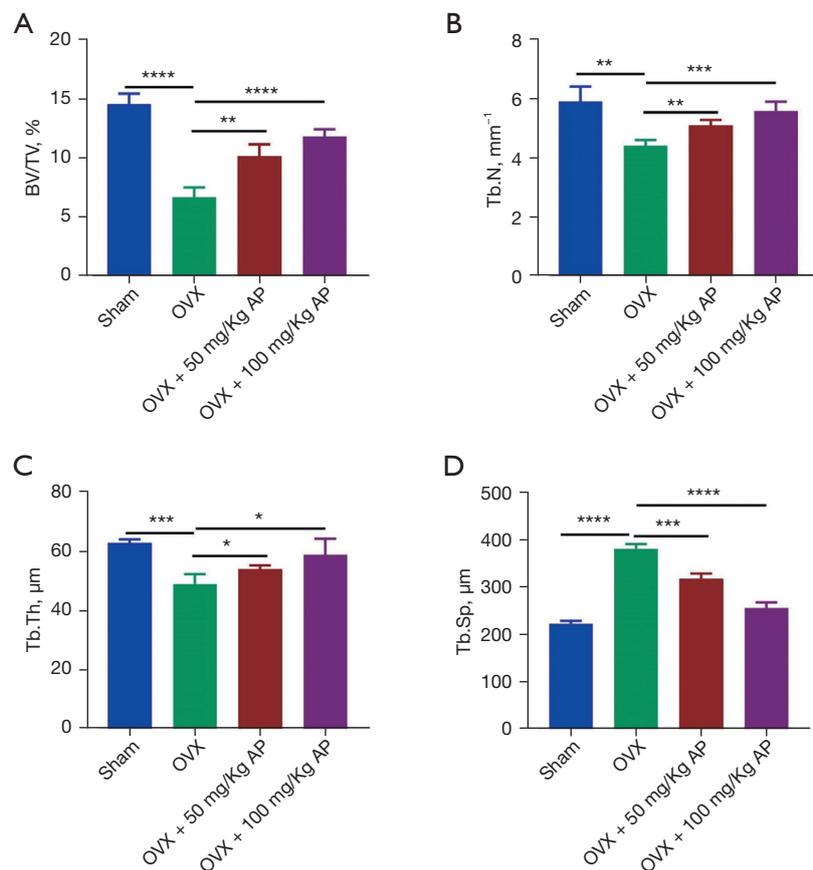
Figure 1 AP treatment and bone loss in osteoporotic mice. (A-D) Quantitative micro-computed tomography analysis of trabecular bone microarchitecture in femurs from sham, OVX, OVX + 50 mg/kg AP and OVX + 100 mg/kg AP groups of mice. n=6 per group. Data are presented as mean ± SD. *, $P<0.05$; **, $P<0.01$; ***, $P<0.001$; ****, $P<0.0001$. AP, Andrographis paniculata; BV/TV, bone volume/tissue volume; Tb.N, trabecular number; Tb.Th, trabecular thickness; Tb.Sp, trabecular separation; OVX, Ovariectomy; SD, standard deviation.

of terminal osteoblastic differentiation, including runt-related transcription factor 2 (*Runx2*), *Osterix* and alkaline phosphatase (*ALP*), play key roles in the osteogenesis of BMSCs and exhibit much higher expression levels (26-28). As shown by qRT-PCR analysis, compared with BMSCs from the sham group, those derived from OVX-induced osteoporotic mice demonstrated significantly decreased expression levels of the osteoblast marker genes (*Runx2*, *Osterix* and *ALP*) (*Figure 4A-4C*). The reduced expressions of *Runx2*, *Osterix* and *ALP* were upregulated by AP administered at 5, 10 and 20 μM, and expression peaked at 20 μM (*Figure 4A-4C*). Taken together, these data suggested that AP beneficially affected osteoblast maturation in OVX-induced estrogen deficiency-related osteoporotic mice.

Effect of AP on osteoporosis-induced fat accumulation of BMSCs

To detect the effect of AP on BMSCs as a functional investigation, BMSCs from OVX-induced osteoporotic mice were treated with AP at 5, 10 and 20 μM and subsequent induction of adipogenic differentiation. After 16 days of differentiation, the induced adipocytes were stained with ORO. As shown in *Figure 5A*, BMSCs from the OVX group exhibited more lipid droplet formation than those form the sham group (*Figure 5A,5B*). The amount of lipid was reversed by all three concentrations of AP (*Figure 5A,5B*).

We also performed qRT-PCR analysis of the expression of master transcription factors during adipogenesis.
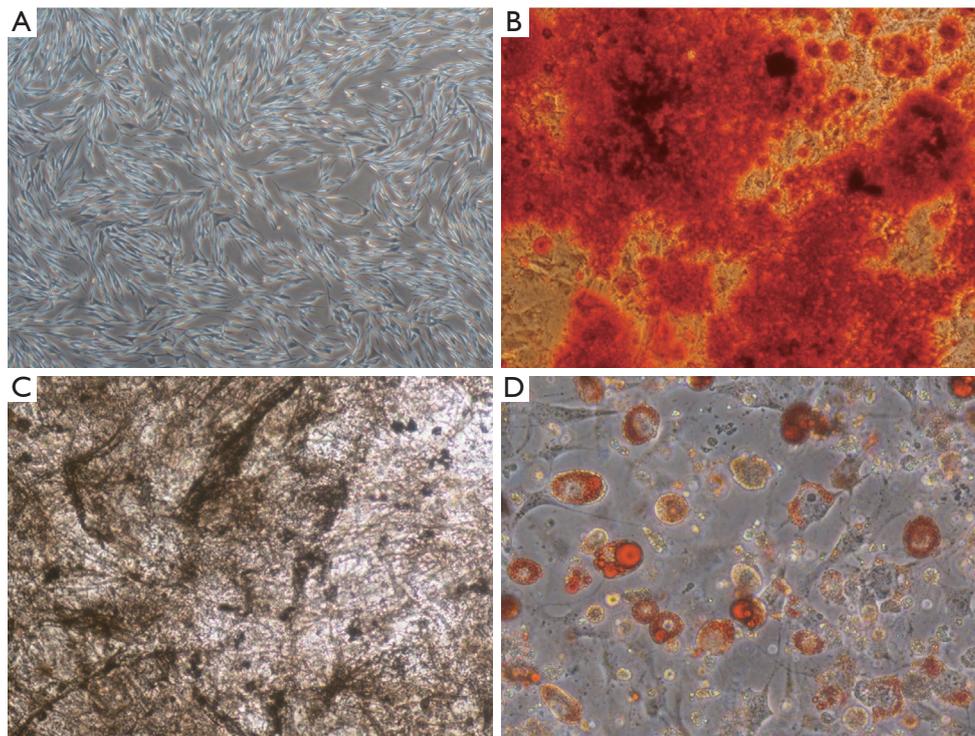
Figure 2 Characterization of BMSCs. (A) Morphology of BMSCs observed by light microscope (×40). (B-D) Differentiation capability of BMSCs into osteoblasts and adipocytes evaluated by Alizarin Red S staining (B: ×100), alkaline phosphatase staining (C: ×100) and Oil Red O staining (D: ×200). BMSCs, bone marrow mesenchymal stem cells.
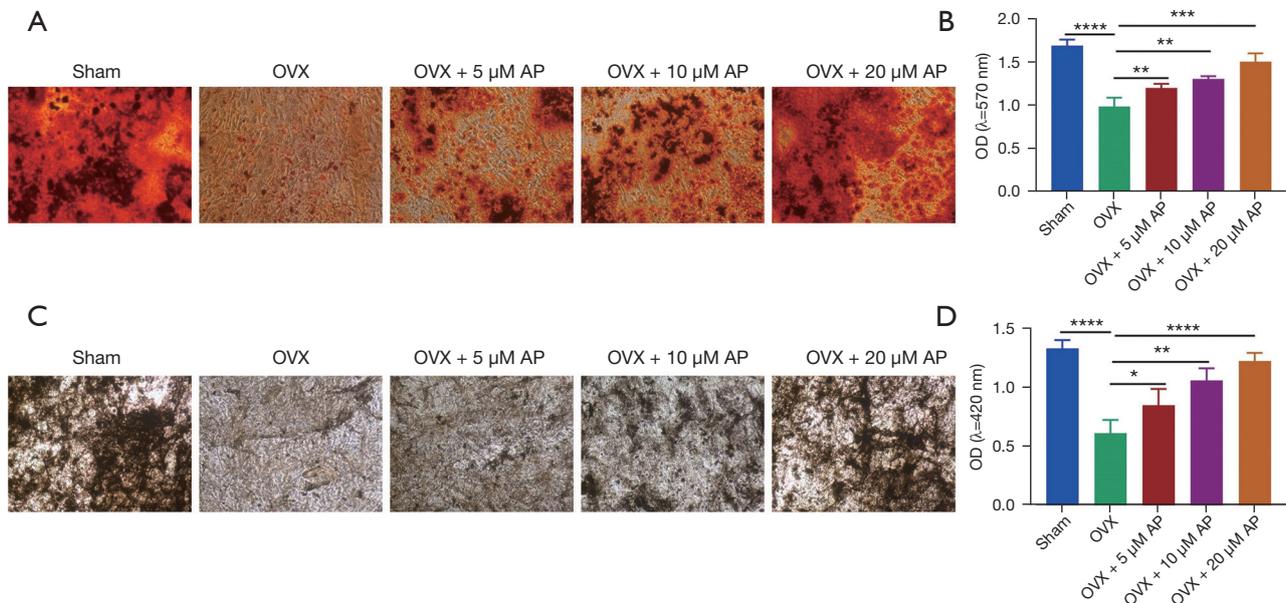
Figure 3 AP and osteogenic differentiation of BMSCs in osteoporotic mice. (A) ARS staining of BMSCs treated with AP on day 14 of differentiation (×100); (B) histograms of quantification of ARS staining; (C) ALP staining of BMSCs after AP treatment (×100); (D) quantification analysis of ALP staining. Data are presented as mean ± SD. *, $P<0.05$; **, $P<0.01$; ***, $P<0.001$; ****, $P<0.0001$. OD, optical density; AP, *Androgaphis paniculata*; BMSCs, bone marrow mesenchymal stem cells; ARS, alizarin Red S; ALP, alkaline phosphatase; SD, standard deviation.
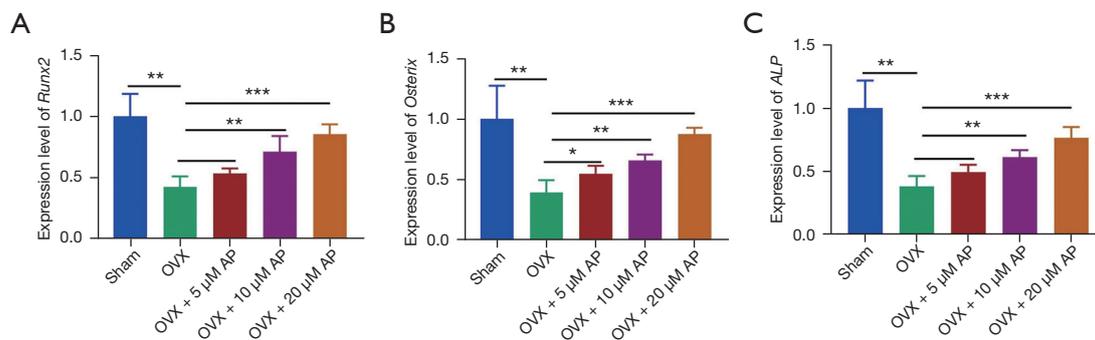
Figure 4 AP treatment and mRNA expression of osteoblastic marker genes of BMSCs in osteoporotic mice. (A-C) Relative mRNA expression of the osteoblastic genes: *Runx2* (A), *Osterix* (B) and *ALP* (C) measured by qRT-PCR analysis on day 14 of osteogenic induction in BMSCs treated with AP. Data are presented as mean ± SD. *, $P<0.05$; **, $P<0.01$; ***, $P<0.001$. AP, *Androgrphis paniculata*; BMSCs, bone marrow mesenchymal stem cells; qRT-PCR, quantitative real-time polymerase chain reaction; *ALP*, alkaline phosphatase; *Runx2*, runt-related transcription factor 2.
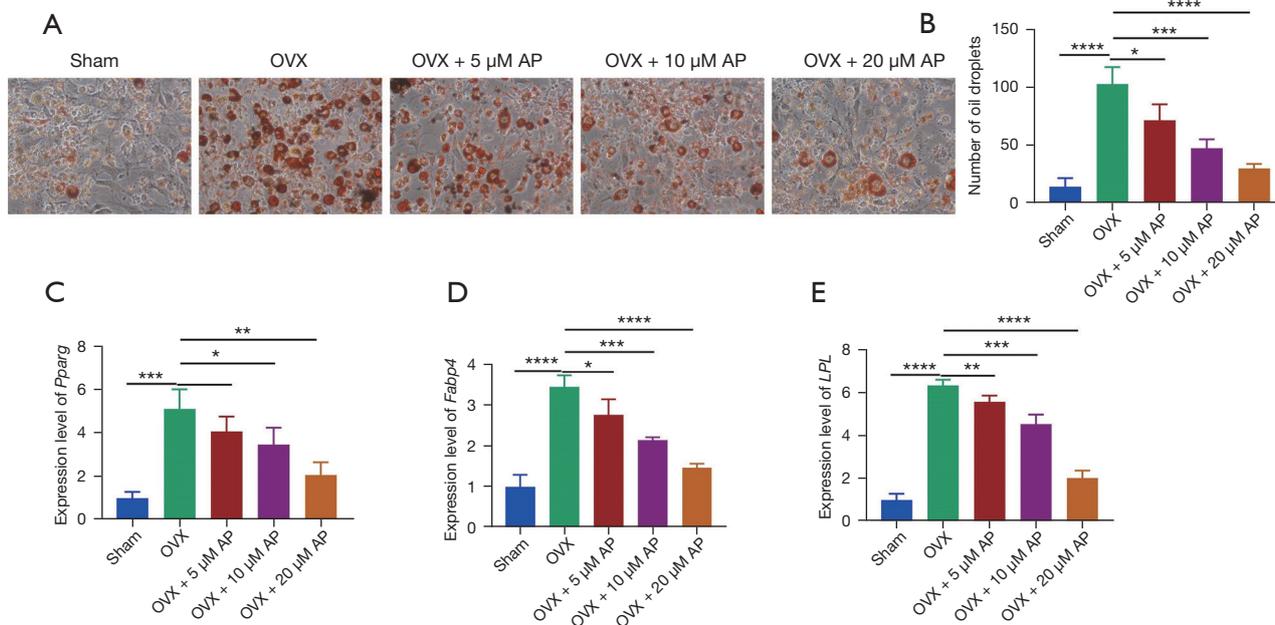
Figure 5 Effect of AP on adipogenic differentiation of BMSCs from osteoporotic mice. (A) Representative images of ORO staining of lipid droplets of BMSCs in the presence of AP (×200); (B) quantification analysis of ORO staining; (C-E) relative levels adipogenic gene markers: *Pparg* (C), *Fabp4* (E) and *LPL* (E), were measured by qRT-PCR in BMSCs induced to differentiate into adipocytes for 16 days. Data are presented as mean ± SD. *, $P<0.05$; **, $P<0.01$; ***, $P<0.001$; ****, $P<0.0001$. OVX, ovariectomy; AP, *Androgrphis paniculata*; BMSCs, bone marrow mesenchymal stem cells; *Fabp4*, fatty acid binding protein 4; *Pparg*, peroxisome proliferator activated receptor-g; *LPL*, lipoprotein lipase; ORO, Oil Red O; qRT-PCR, quantitative real-time polymerase chain reaction.

The mRNA levels of three important adipocyte genes, peroxisome proliferator activated receptor-g (*Pparg*), fatty acid binding protein 4 (*Fabp4*) and lipoprotein lipase (LPL), were upregulated in BMSCs from osteoporotic mice (*Figure 5C-5E*). After the BMSCs derived from osteoporotic mice were treated with AP, the pro-adipogenic effects of osteoporosis were abolished, indicating that AP can target BMSCs to inhibit adipocyte formation (*Figure 5C-5E*). Taken together, these findings suggested that AP impaired osteoporosis-induced fat accumulation of BMSCs.

Discussion

Osteoporosis is a systemic skeletal disorder characterized by reduced bone mass, impaired microstructure of bone tissue and increased bone fragility and risk of fracture (29,30). Currently, some effective treatments are used for osteoporosis. Anti-resorptive methods, such as bisphosphonates and denosumab, could improve the bone mineral density (BMD) and decrease the risks of osteoporotic fractures by about 20% to 70%. Bone-forming and dual-action therapies can promote the bone formation and improve the BMD and the effects are better than the anti-resorptive methods. It has been demonstrated that these two current treatments are superior to anti-resorptive methods in the prevention of fractures in osteoporotic patients. Bone-forming methods and dual-action methods should be performed after the anti-resorptive treatments to reduce the fracture risks. The BMD gains in osteoporotic patients treated with bone-forming and dual-action treatments are much greater in patients treated with anti-resorptive treatments. However, the anti-fracture efficacy seems to be preserved. Osteoporosis is a type of chronic condition, which might need long-term management plans with personalized approaches to treatment.

Disruption in bone remodeling resulting in increased adipogenesis and reduced osteogenesis of BMSCs can lead to osteoporosis (31). BMSCs can differentiate into a variety of cell types, such as osteoblasts, chondrocytes and adipocytes (32). Reports have indicated that BMSCs exhibit decreased abilities of osteogenic differentiation when osteoporosis occurs (33,34). In the current study, BMSCs isolated from OVX-induced estrogen deficiency-related osteoporosis mice exhibited decreased osteogenic and increased adipogenic potentials, which was consistent with results from a previous study (32). Thus, the application of BMSCs in bone regeneration and targeting BMSCs fate is a promising strategy to cure bone loss-related diseases such as osteoporosis.

There is mounting evidence of the biological functions of AP, such as anticancer, anti-inflammatory, antimalarial, antimicrobial, antioxidant, cardioprotective and immunomodulatory activities (35-37), but not of its role in estrogen deficiency-related osteoporosis. Our study results verified the characteristics of accelerated bone loss in OVX-induced estrogen deficiency-related osteoporotic mice and showed that it could be counteracted by AP treatment. Additional analysis indicated that AP reversed the decreased mineralization capability and impaired the osteoporosis-induced fat accumulation of BMSCs from osteoporotic mice. Our study provides the first demonstration that AP affected the imbalance between osteogenesis and adipogenesis of BMSCs from osteoporotic mice.

Conclusions

In summary, AP treatment prevented both the bone loss and impaired osteogenesis of BMSCs in estrogen deficiency-related osteoporotic mice. AP also reversed the increased adipogenesis of BMSCs from osteoporotic mice. These findings strongly suggested that AP might prevent the development of osteoporosis by regulating the osteogenesis and adipogenesis of BMSCs. AP shows promise as a treatment for osteoporosis, but more research into the regulatory mechanism is needed.

Footnote

Reporting Checklist: The authors have completed the ARRIVE reporting checklist. Available at https://atm.amegroups.com/article/view/10.21037/atm-22-1121/rc

Data Sharing Statement: Available at https://atm.amegroups.

com/article/view/10.21037/atm-22-1121/dss

Conflicts of Interest: All authors have completed the ICMJE uniform disclosure form (available at https://atm.amegroups.com/article/view/10.21037/atm-22-1121/coif). The authors have no conflicts of interest to declare.

Ethical Statement: The authors are accountable for all aspects of the work in ensuring that questions related to the accuracy or integrity of any part of the work are appropriately investigated and resolved. Animal experiments were performed under a project license (No. 2021121) granted by the Ethics Committee of Tianjin Hospital, in compliance with institutional guidelines for the care and use of animals.

Open Access Statement: This is an Open Access article distributed in accordance with the Creative Commons Attribution-NonCommercial-NoDerivs 4.0 International License (CC BY-NC-ND 4.0), which permits the non-commercial replication and distribution of the article with the strict proviso that no changes or edits are made and the original work is properly cited (including links to both the formal publication through the relevant DOI and the license). See: https://creativecommons.org/licenses/by-nc-nd/4.0/.

References

1. Li Y, Meng L, Zhao B. The roles of N6-methyladenosine methylation in the regulation of bone development, bone remodeling and osteoporosis. Pharmacol Ther 2022;238:108174.
2. Li Y, Hao W, Guan J, et al. Relationship between indices of circulating blood cells and bone homeostasis in osteoporosis. Front Endocrinol (Lausanne) 2022;13:965290.
3. Shen G, Ren H, Shang Q, et al. Foxf1 knockdown promotes BMSC osteogenesis in part by activating the Wnt/β-catenin signalling pathway and prevents ovariectomy-induced bone loss. EBioMedicine 2020;52:102626.
4. Zhang H, Wang L, Wen S, et al. Magnetic resonance imaging tracking and assessing repair function of the bone marrow mesenchymal stem cells transplantation in a rat model of spinal cord injury. Oncotarget 2017;8:58985-99.
5. Lin Z, He H, Wang M, et al. MicroRNA-130a controls bone marrow mesenchymal stem cell differentiation towards the osteoblastic and adipogenic fate. Cell Prolif 2019;52:e12688.
6. Meyer MB, Benkusky NA, Sen B, et al. Epigenetic Plasticity Drives Adipogenic and Osteogenic Differentiation of Marrow-derived Mesenchymal Stem Cells. J Biol Chem 2016;291:17829-47.
7. Mohamed-Ahmed S, Fristad I, Lie SA, et al. Adipose-derived and bone marrow mesenchymal stem cells: a donor-matched comparison. Stem Cell Res Ther 2018;9:168.
8. Qi M, Zhang L, Ma Y, et al. Autophagy Maintains the Function of Bone Marrow Mesenchymal Stem Cells to Prevent Estrogen Deficiency-Induced Osteoporosis. Theranostics 2017;7:4498-516.
9. Zhou R, Chen F, Liu H, et al. Berberine ameliorates the LPS-induced imbalance of osteogenic and adipogenic differentiation in rat bone marrow-derived mesenchymal stem cells. Mol Med Rep 2021;23:350.
10. Li Y, Jin D, Xie W, et al. PPAR-γ and Wnt Regulate the Differentiation of MSCs into Adipocytes and Osteoblasts Respectively. Curr Stem Cell Res Ther 2018;13:185-92.
11. Gao M, Zhang Z, Sun J, et al. The roles of circRNA-miRNA-mRNA networks in the development and treatment of osteoporosis. Front Endocrinol (Lausanne) 2022;13:945310.
12. Guo Q, Chen Y, Guo L, et al. miR-23a/b regulates the balance between osteoblast and adipocyte differentiation in bone marrow mesenchymal stem cells. Bone Res 2016;4:16022.
13. Qadir A, Liang S, Wu Z, et al. Senile Osteoporosis: The Involvement of Differentiation and Senescence of Bone Marrow Stromal Cells. Int J Mol Sci 2020;21:349.
14. Kumar S, Singh B, Bajpai V. Andrographis paniculata (Burm.f.) Nees: Traditional uses, phytochemistry, pharmacological properties and quality control/quality assurance. J Ethnopharmacol 2021;275:114054.
15. Widjajakusuma EC, Jonosewojo A, Hendriati L, et al. Phytochemical screening and preliminary clinical trials of the aqueous extract mixture of Andrographis paniculata (Burm. f.) Wall. ex Nees and Syzygium polyanthum (Wight.) Walp leaves in metformin treated patients with type 2 diabetes. Phytomedicine 2019;55:137-47.
16. Rafi M, Devi AF, Syafitri UD, et al. Classification of Andrographis paniculata extracts by solvent extraction using HPLC fingerprint and chemometric analysis. BMC Res Notes 2020;13:56.
17. Rajagopal K, Varakumar P, Baliwada A, et al. Activity of phytochemical constituents of Curcuma longa (turmeric) and Andrographis paniculata against coronavirus

(COVID-19): an in silico approach. Futur J Pharm Sci 2020;6:104.

18. Luo S, Li H, Liu J, et al. Andrographolide ameliorates oxidative stress, inflammation and histological outcome in complete Freund's adjuvant-induced arthritis. Chem Biol Interact 2020;319:108984.

19. Kulsirirat T, Honsawek S, Takeda-Morishita M, et al. The Effects of Andrographolide on the Enhancement of Chondrogenesis and Osteogenesis in Human Suprapatellar Fat Pad Derived Mesenchymal Stem Cells. Molecules 2021;26:1831.

20. Yang F, Yang L, Li Y, et al. Melatonin protects bone marrow mesenchymal stem cells against iron overload-induced aberrant differentiation and senescence. J Pineal Res 2017.

21. Yang L, Li Y, Gong R, et al. The Long Non-coding RNA-ORLNC1 Regulates Bone Mass by Directing Mesenchymal Stem Cell Fate. Mol Ther 2019;27:394-410.

22. Zhao X, Chen C, Wei Y, et al. Novel mutations of COL4A3, COL4A4, and COL4A5 genes in Chinese patients with Alport Syndrome using next generation sequence technique. Mol Genet Genomic Med 2019;7:e653.

23. Lu GD, Cheng P, Liu T, et al. BMSC-Derived Exosomal miR-29a Promotes Angiogenesis and Osteogenesis. Front Cell Dev Biol 2020;8:608521.

24. Hu H, Zhao C, Zhang P, et al. miR-26b modulates OA induced BMSC osteogenesis through regulating GSK3β/β-catenin pathway. Exp Mol Pathol 2019;107:158-64.

25. Li Z, Zhao H, Chu S, et al. miR-124-3p promotes BMSC osteogenesis via suppressing the GSK-3β/β-catenin signaling pathway in diabetic osteoporosis rats. In Vitro Cell Dev Biol Anim 2020;56:723-34.

26. Deng L, Hu G, Jin L, et al. Involvement of microRNA-23b in TNF-α-reduced BMSC osteogenic differentiation via targeting runx2. J Bone Miner Metab 2018;36:648-60.

27. Wang L, Lu WG, Shi J, et al. Anti-osteoporotic effects of tetramethylpyrazine via promoting osteogenic differentiation and inhibiting osteoclast formation. Mol Med Rep 2017;16:8307-14.

28. Sun Y, Zhu Y, Liu X, et al. Morroniside attenuates high glucose-induced BMSC dysfunction by regulating the Glo1/AGE/RAGE axis. Cell Prolif 2020;53:e12866.

29. Wu W, Fu J, Gu Y, et al. JAK2/STAT3 regulates estrogen-related senescence of bone marrow stem cells. J Endocrinol 2020;245:141-53.

30. Guo R, Li B, Zeng Z, et al. Thoracolumbar kyphosis in postmenopausal osteoporosis patients without vertebral compression fractures. Ann Transl Med 2022;10:52.

31. Maria S, Samsonraj RM, Munmun F, et al. Biological effects of melatonin on osteoblast/osteoclast cocultures, bone, and quality of life: Implications of a role for MT2 melatonin receptors, MEK1/2, and MEK5 in melatonin-mediated osteoblastogenesis. J Pineal Res 2018;64:10.1111/jpi.12465.

32. Xu R, Fu Z, Liu X, et al. Transplantation of osteoporotic bone marrow stromal cells rejuvenated by the overexpression of SATB2 prevents alveolar bone loss in ovariectomized rats. Exp Gerontol 2016;84:71-9.

33. Zhou L, Poon CC, Wong KY, et al. Icariin ameliorates estrogen-deficiency induced bone loss by enhancing IGF-I signaling via its crosstalk with non-genomic ERα signaling. Phytomedicine 2021;82:153413.

34. Wu T, Sun J, Tan L, et al. Enhanced osteogenesis and therapy of osteoporosis using simvastatin loaded hybrid system. Bioact Mater 2020;5:348-57.

35. Islam MT, Ali ES, Uddin SJ, et al. Andrographolide, a diterpene lactone from Andrographis paniculata and its therapeutic promises in cancer. Cancer Lett 2018;420:129-45.

36. Rafi M, Karomah AH, Heryanto R, et al. Metabolite profiling of Andrographis paniculata leaves and stem extract using UHPLC-Orbitrap-MS/MS. Nat Prod Res 2022;36:625-9.

37. Adedayo BC, Jesubowale OS, Adebayo AA, et al. Effect of Andrographis paniculata leaves extract on neurobehavioral and biochemical indices in scopolamine-induced amnesic rats. J Food Biochem 2021;45:e13280.

(English Language Editor: K. Brown)